Optimal Distributed Nonlinear Battery Control

Alper Sinan Akyurek, *Member, IEEE,* Tajana Simunic Rosing, *Senior Member, IEEE*

***Abstract*—Energy storage plays a more important role than ever before, due to the transition to smart grid along with higher penetration of renewable resources. In this paper, we describe our optimal nonlinear battery control algorithm that can handle multiple batteries connected to the grid in a distributed and cost-optimal fashion, while maintaining low complexity of $O(N^2)$. In contrast to the state-of-the-art, we use a high accuracy nonlinear battery model with 2% error. We present three distributed solutions: 1) Circular negotiation ring, providing convergence rates independent of number of batteries, 2) Mean circular negotiation ring, converging very quickly for a low number of batteries, 3) Bisection method has a convergence rate independent of battery capacities. We compare our algorithm to the state-of-the-art and show that we can decrease the utility cost of an actual building by up to 50% compared to the batteryless case, by 30% over the load-following heuristic and by 60% over a state-of-the-art optimal control algorithm designed using a linear battery model. For a constant load profile, optimal linear control incurs costs higher by 150% for MPC and 250% for single trajectory solutions, than our algorithm.**

I. Introduction

Smart grid brings concepts of load automation and distributed generation. The current structure of the power grid is designed to have generation handled by large centralized generators and the consumption to be within predictable limits. Small mismatches in generation and consumption are balanced through multiple controllers and immediate changes are damped by the inertia of a spinning mechanical generator [1].

On the load side, automation transforms the predictable, average daily human behavior into a more complex function due to load shifting, two-way communication, pricing mechanisms [2] and demand response [3]. Renewable distributed generation brings new challenges with it. There are many forecasting algorithms for wind [4] and solar [5] energy, but errors are inevitable due to their highly varying nature.

Energy storage devices (ESDs) are used either as stand-alone batteries [6] or indirectly as a part of Electrical Vehicles (EVs), also known as Vehicle to Grid (V2G) [7]. The advantage of batteries is their flexibility to be used as either load or generator at adjustable power levels. The phase of the injected power can be adjusted to control the reactive power [8]. The power output can be adjusted for voltage stability [9]. Disadvantages of batteries include the high capital costs and the nonlinear characteristics that makes the profitability harder to predict [10].

In this work, we target the finite horizon optimal economic dispatch problem of how multiple inherently nonlinear batteries with nonlinear power and degradation characteristics connected to the grid should be used and controlled, such that the aggregate electricity cost of a distribution circuit, such as an energy sharing neighborhood or a microgrid, is minimized. We obtain the optimal timeseries solution of each battery's power consumption to minimize the aggregate costs under different electricity cost schemes. We consider both centralized and distributed implementations. Our main contributions are: 1) We use a nonlinear battery model for lithium-ion batteries to describe charging/discharging and degradation characteristics and find a low-complexity optimal centralized solution for a generalized cost function using dynamic programming. The centralized solution is converted into distributed algorithms without any loss of optimality. The region of convergence and the convergence rates of the solutions are studied and verified. 2) We obtain 50% cost reduction compared to the batteryless case and 30% improvement over the state-of-the-art battery management technique of load-following. 3) We provide a comparison with an optimal solution based on a linear battery model, and show that if it were to be used on a realistic nonlinear battery, it would deviate by up to 60% in terms of cost reduction from the nonlinear optimal solution. For a constant profile, we show that this deviation can be higher than 150%. This is caused by the accumulation of model errors in time, resulting in premature constraint violations. 4) We provide a voltage stability study for a real neighborhood circuit, where we show that we can decrease the maximum voltage deviation by up to 45% using multiple batteries in the neighborhood, improving stability.

A. Akyurek and T. Rosing are with the Department of Electrical and Computer Engineering, University of California, San Diego, CA, 92093 USA, e-mail: {aakyurek, tajana}@ucsd.edu

II. Related Work

Increased penetration of renewable resources with rapid variations and increased usage of electric vehicles shifted many studies towards energy storage systems and their control. We divide the literature into battery *control* and *modeling* the electrical behavior of different battery systems. There is a growing gap between the more complex and accurate battery models and, fast and optimal control strategies. Complex battery models try to model every detail of internal battery characteristics, making it practically impossible to implement feasible large scale control algorithms. On the other hand, large scale control algorithms oversimplify the battery models in order to obtain optimal solutions for battery control problems.

A. Related Work on Battery Control

Batteries can smooth out the intermittent nature of the renewable sources and decrease the peak power usage of the system by charging at non-peak hours and discharging at peak hours [11]. Different kinds of energy storage techniques currently used in smart grid development is given in [12]; examples range from 34MW Sodium Sulfur down to 25kW residential area batteries. For a good summary of current

energy storage uses, see [13], [14], [15]. In [16], a price-based energy management solution is proposed for a system with photovoltaics (PV) and batteries minimizing the financial loss. In [11], ramp rate control is proposed, which holds the rate of change in PV power output within a stable boundary. In [17], authors determine (dis)charging regimes for frequency and voltage regulation based on a threshold.

In order to obtain the optimal solution, existing papers in the literature focus on linearized battery models to simplify the constraints of the optimization problem. In [18], extensive work was done on the stability, peak shaving and capital cost performances of batteries using a linear battery model with quadratic programming (QP). The authors show for a residential area with PV that batteries increase the integration of PV, improve stability and simplify the over-voltage problem. In [19], the authors look into the problem of coordinated electric vehicle charging. The optimization problem is defined using a linear battery model and a quadratic cost function, representing the market balance and user discomfort. For further information on electric vehicles, please see the survey [20]. In [21], the authors approach the battery control problem from a DC microgrid perspective. The battery is modeled such that the nonlinear connection between the battery voltage and battery power is explicitly accurate. This connection is then leveraged in a hardware implementation to control the voltage levels at the utility substation transformer. A recent paper [22] considers a residential neighborhood with PV and linearly modeled batteries. The authors propose 4 different algorithms: a heuristic, centralized model predictive control (MPC), a decentralized MPC and a novel market maker distributed MPC. In all cases, the objective is to flatten out the aggregated power profile drawn from the grid.

B. Related Work on Battery Modeling

The simplest and most frequently used battery model is linear, where the change in battery state of charge (SoC) is a linear function of the battery's terminal power consumption. This is expressed in (1), where $\eta_C < 1$ is the battery efficiency constant for charging and $\eta_D = \eta_C^{-1} > 1$ for discharging. SU is the charge capacity of the battery.

$$\text{State of Charge}(t) = \text{SoC}(0) + \frac{\eta_{C,D}}{SU} \int_{t'=0}^{t} \text{Battery Power}(t')dt' \tag{1}$$

However, it is shown in [23] that the linear model has high errors for high discharge currents. Since renewable resources are intermittent and have rapid variations, high currents are frequent in grid related uses. There are many accurate and complex battery models proposed in the literature. See [24] for a comprehensive survey and [25] for an overview on different levels of degradation models.

In [26], the authors introduce a circuit based model. The paper introduces two degradation models based on temperature, self discharge and capacity fading, along with the consumption values. A Ph.D. thesis [27] models the battery (dis)charging memory effects and degradation effects based on the internal chemistry of lithium-ion batteries. Many different cycle testing cases are required to create the detailed model. The Riso Report [28] further discusses degradation effects based on the battery's consumption values in the form of analytic functions. The model is based on the internal chemistry of the battery. National Renewable Energy Laboratory (NREL) has a report [29] that models the battery from the perspectives of capacity degradation, depth of discharge memory effect and nonlinear charging and discharging characteristics. All properties are provided in the form of analytic functions making it easier to include within mathematical optimization. In [30], an analytic model is provided for degradation, including temperature, depth of discharge and state of charge based capacity fading. The authors use a linear SoC model along with the degradation model to solve an economic dispatch problem in [31]. In [32] the authors provide a state of charge and depth of discharge based degradation model. This is then used with a linear state of charge model to solve an electric vehicle optimization problem. Effect of temperature is neglected based on steady operating temperature conditions.

As opposed to analytics based model, there are also degradation estimation methods based on the internal physics. In [33], [34], [35] and [36], the unwanted chemical side reactions inside a lithium ion battery are modeled to obtain particle level aging estimation for very accurate degradation modeling during design time. These include recoverable and unrecoverable fading effects. In [37] a cell level optimization is described based on 2D physics based model. However, for larger scale and real time applications these models become very complex.

As seen in previous works, modeling the battery is a tradeoff between control quality and computational simplicity. We consider two aspects of the battery; state of charge and state of health (SoH). SoC defines the charge level of the battery. SoH is the measure of battery's charge holding capacity degradation. SoH declines slowly from 1 (brand new) to 0 (completely dead). We could include internal chemical reactions, physics and hysteresis effects to obtain a very accurate complex battery model, but the solution complexity increases by multiple orders of magnitude. In this work, we discard the hysteresis effects to keep the computational complexity to $O(N^2)$, but we retain the nonlinearity in SoC and SoH for our battery model, with an error of only 2% compared to empirical data (Section V).

The widely used linear model, shown in (1), defines a linear SoC dependence that fails to represent the nonlinearity at high discharge currents, known as the Peukert's effect. Previous works show that linear models ignoring this effect can have an error as high as 43% [23]. Our SoC model, based on [23][27][38], is shown in (2), which states that higher discharge currents lead to an exponentially smaller effective capacity (SoC). α is the Peukert exponent and describes the exponential nonlinearity of the SoC relation.

$$\text{SoC}(t) = \text{SoC}(0) + \frac{1}{SU} \int_{t'=0}^{t} \text{Battery Power}^{\alpha}(t')dt', \alpha > 1 \tag{2}$$

As an example, if the battery output power is doubled, the amount of charge lost is increased by 2.2x for $\alpha = 1.15$.

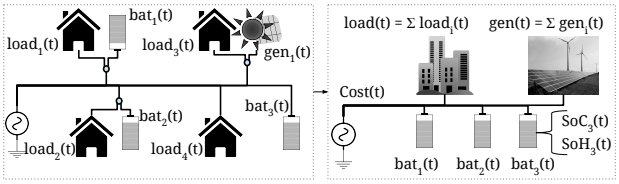

Figure 1. System model overview and load aggregation

Solutions neglecting this effect can be misleadingly biased towards the use of high discharge currents causing accumulative control errors of more than 150% as shown in Section V. From the SoH perspective, the linear battery model assumes no degradation, keeping SoH$=1$. A model without degradation would neglect aging and loss in capital value of the battery completely. Although degradation occurs slowly in time, the effect is noticeable over longer intervals. The SoH model for lithium-ion batteries used in this work is based on discharge throughput degradation [28][29] and, temperature and state of charge degradation [30][31], is shown in (3).

$$\begin{aligned}\text{SoH}(t) &= \text{SoH}(0) \\ &- \left[\int_{t'=0}^{t} \beta e^{\gamma \text{ Batt. Pwr.}(t')-\theta} dt'\right] - [\phi_1 \text{SoC}_{\text{avg}}(t) + \phi_2] \\ &- \left[\int_{t'=0}^{t} \sigma_1 e^{-\sigma_2(T_{amb}+\sigma_3|\text{Batt. Pwr.}|)^{-1}} dt' + \sigma_4(T_{amb})\right] \end{aligned} \quad (3)$$

The first bracket expression states that the SoH degradation is exponential with the discharge throughput and linearly related to the discharge amount for a fixed time interval. β is the exponential scale of degradation, γ is the linear modification from discharge amount to Amperes-Hour (AH) discharge throughput and θ is the inefficiency coefficient for converting an amount of charge into actually stored charge. These parameters are device dependent and can be obtained from either battery data sheets that provide depth of discharge and cycle life results or from experimental results. More information on this process is provided in [29]. The second bracket expression is degradation due to the SoC level, modeled linearly in [30]. The coefficients in the original model have been converted to the time resolution used in this work and are obtained by fitting to the experimental measurements in [39]. The last bracket expression is the degradation due to temperature. It models the temperature change in the battery linearly through a thermal resistance and adjusts the degradation with respect to the current ambient temperature (T_{amb}). The coefficients in the original model [31] have been combined into ambient temperature dependent function of σ_4 and constants of $\sigma 1, \sigma_2$ and σ_3 for convenience in representation. These coefficients are obtained by fitting to the experimental measurements in [39]. Throughout this work, we have used lithium-iron-phosphate battery chemistry for all model fits, case studies and, accuracy, complexity and performance results. The parameters are $\alpha = 1.15, \beta = 25, \gamma = 0.017, \theta = 19.9, \sigma_1 = 1.4 \times 10^{-4}, \sigma_2 = -75, \sigma_3 = 0.1, \phi_1 = -10^{-3}, \phi_2 = 10^{-8}$. However, the underlying optimal control solution is valid for different analytic battery models using the same control solution. The main purpose of this work is not to advance the literature on battery models, but rather provide a novel optimal nonlinear control strategy capable of accounting for nonlinear battery models to increase accuracy.

III. Optimal Centralized Nonlinear Battery Control

A. System Model

The main goal of this work is to solve the optimal economic dispatch problem, where we solve for the power level of each grid-connected battery at every time interval, such that the resulting power profiles are cost-optimal in a finite horizon. Our system model consists of a circuit with 3 types of devices: loads, distributed generators and batteries. We aggregate all consumption and generation values into a single time-series, but leave batteries separate to study the effect of nonlinear battery characteristics. We assume that the line-losses in our aggregate model are constant, resulting in a mean absolute error of only 0.8% as shown in Section V. Aggregation is widely used in the literature for battery control problems [17][19][22]. Note that a battery at a particular location can physically consist of a battery bank, however we refer to them as batteries for simplicity in notation throughout this work.

We begin our formulation by dividing time into discrete intervals of equal length. Any variable $x_{n,t}$ represents the quantity x for the n^{th} battery at the t^{th} time interval. *load*, *gen* and *bat* represent consumption, generation and battery consumption values, respectively. We jointly represent the total load and generation as: $p_t = \sum_k \text{load}_{k,t} + \sum_m \text{gen}_{m,t}$, since they are not controllable. The overview of the system is shown in Figure 1. Next, we define constraints to represent the battery's physical nature: 1) Power Limit: The discharge and charge power of a battery is limited, thus the energy consumption per interval is also bounded by $L_n \leq \text{bat}_{n,t} \leq U_n, \forall n, t$. 2) Charge Limit: SoC, is upper-limited by a value depending on the health of the battery. A lower limit is also enforced to avoid quick lifetime depletion, represented by $SL_n \leq SoC_{n,t} \leq SU_n, \forall n, t$. Each battery model has three state variables: energy consumption $\text{bat}_{n,t}$, state of charge $SoC_{n,t}$ and state of health $SoH_{n,t}$. Only $\text{bat}_{n,t}$ is independently controllable, whereas SoC and SoH dependent on the energy consumption of the current interval and their previous values, respectively. Our battery model uses the discrete time forms of (2) and (3):

$$\text{SoC}_{n,t+1} = \text{SoC}_{n,t} + \text{soc}_{n,t} = \text{SoC}_{n,t} + \frac{1}{SU_n}(\text{bat}_{n,t})^{\alpha_n} \quad (4)$$

$$\begin{aligned}\text{SoH}_{n,t+1} &= \text{SoH}_{n,t} + \text{soh}_{n,t} \\ &= \text{SoH}_{n,t} - \beta_n e^{(\gamma_n|\text{bat}_{n,t}|-\theta_n)} - \frac{\phi_{n,1}}{SU_n}(\text{bat}_{n,t})^{\alpha_n} \\ &-\phi_{n,2} - \sigma_{n,1} e^{-\sigma_{n,2}(T_{amb}+\sigma_{n,3}|\text{bat}_{n,t}|)^{-1}+\sigma_{n,4}(T_{amb})} \end{aligned} \quad (5)$$

In practice SoH is a very slowly varying property. Thus in our solution, we update SoH only over long time intervals (24-hours for simulations).

Table I
KKT MULTIPLIER DEFINITIONS AND REGIONS

	Description	Condition
$A_{n,t}$	Battery n is full at time t	$A_{n,t} > 0$
$B_{n,t}$	Bat. n is empty at time t	$B_{n,t} > 0$
$X_{n,t}$	Bat. n charges with max. power at t	$X_{n,t} > 0$
$Y_{n,t}$	Bat. n discharges with max. power at t	$Y_{n,t} > 0$

B. Problem Formulation

We define two different cost factors: 1) a general memoryless function, C, that depends on the total consumption of the considered loads, generators and batteries (eg. the utility bill of a microgrid) 2) the cost of degradation, which is the loss in the invested capital value. We define K_n as the capital cost of battery n, thus the degradation of the battery at the end of t intervals is defined by: $\text{Deg}_{n,t} = K_n\left(SoH_{n,0} - SoH_{n,t}\right)$. The optimization problem for a finite interval of T is:

$$\min_{\forall b} \sum_n \text{Deg}_{n,T} + \sum_{t=1}^{T} C\left(p_t + \sum_n \text{bat}_{n,t}\right) \text{ s. t.}$$
$$SL_n \leq SU_n \cdot \text{SoC}_{n,t} \leq SU_n, \quad L_n \leq \text{bat}_{n,t} \leq U_n, \forall n \tag{6}$$

We solve this problem using its Lagrangian dual:

$$\begin{aligned}
\mathcal{L} &= \sum_{t=1}^{T} C(p_t + \sum_n \text{bat}_{n,t}) + \sum_n K_n\left(\text{SoH}_{n,0} - \text{SoH}_{n,T}\right) \\
&+ \sum_n \sum_{t=1}^{T} A_{n,t}\left(SU_n \text{SoC}_{n,t} - SU_n\right) \\
&+ \sum_n \sum_{t=1}^{T} B_{n,t}\left(SL_n - SU_n \text{SoC}_{n,t}\right) \\
&+ \sum_n \sum_{t=1}^{T} X_{n,t}\left(\text{bat}_{n,t} - U_n\right) + Y_{n,t}\left(L_n - \text{bat}_{n,t}\right)
\end{aligned} \tag{7}$$

The KKT multipliers defined for the constraints are explained in Table I, along with necessary conditions. Note that constraint functions are convex and we assume C to be also convex to satisfy Slater's condition for strong duality. Using $C_t = C\left(p_t + \sum_m \text{bat}_{m,t}\right)$, $Z_{n,t} = Y_{n,t} - X_{n,t}$ and $\lambda_{n,t} = B_{n,t} - A_{n,t}$, the optimal solution for any interval t is:

$$\frac{\partial C_t}{\partial \text{bat}_{n,t}} = Z_{n,t} + \sum_{t'=1}^{T} \lambda_{n,t'} SU_n \frac{\partial SoC_{n,t'}}{\partial \text{bat}_{n,t}} \tag{8}$$

Two major implications arise from this expression: 1) The equation is independent of past decisions and can be solved using dynamic programming: starting at T and iteratively solving back until $t = 1$. This property becomes the basis of our low complexity solution explained later in this section; 2) The right hand side of (8) depends on a *single* battery, but is equal to a function of the summation of *all* batteries. This becomes the basis of our distributed solution in Section IV.

C. Centralized Solution

Dynamic programming is a high complexity and generalized solution method. To mitigate its disadvantages, we use the sparsity in our specific problem definition to obtain a new low-complexity solution. We use C', soc' and soh' to denote the derivatives of C, soc and soh in (4), and use them in (8):

$$C'_t = Z_{n,t} + SU_n soc'_{n,t} \sum_{t'=t+1}^{T} \lambda_{n,t'} \tag{9}$$

We define the right hand side of the equation as the individual constraint function since it only involves the individual properties of a battery. $Z_{n,t}$ and $\lambda_{n,t}$ variables dictate the state of the battery. A negative $Z_{n,t}$ means the battery is at its discharge power limit, whereas for a positive value the battery is at its charging power limit. $\lambda_{n,t}$ introduces three states: A negative $\lambda_{n,t}$ means that the battery is *empty*, a positive value means the battery is *full* and $\lambda_{n,t} = 0$ means the battery is transitioning from one state to another, thus *transient*. We normalize (9) by $soc'_{n,t}$ and take a finite difference at time t to obtain $\lambda_{n,t}$:

$$\lambda_{n,t} = \frac{C'_{t-1} - Z_{n,t-1}}{SU_n soc'_{n,t-1}} - \frac{C'_t - Z_{n,t}}{SU_n soc'_{n,t}}, \forall n, t \tag{10}$$

Equation (10) dictates the state of every battery. For a transient state ($\lambda = 0$), if the battery model were linear, the denominator would be 1, resulting in a solution of constant cost profile, whereas in our nonlinear solution, the *cost per used charge* is kept constant. For a full state ($\lambda > 0$), the cost per used charge should be decreasing and for an empty state ($\lambda < 0$), increasing. Most importantly, this equality dictates that all batteries must have the same state at the same time for the optimal solution. We prove this by contradiction. Assume that battery n is in a transient state, while battery m is full:

$$\frac{C'_{t-1}}{SU_n soc'_{n,t-1}} = \frac{C'_t}{SU_n soc'_{n,t}} = \frac{C'_{t+1}}{SU_n soc'_{n,t+1}} \quad \text{transient}$$
$$\frac{C'_{t-1}}{SU_m soc'_{m,t-1}} > \frac{C'_t}{SU_m soc'_{m,t}} > \frac{C'_{t+1}}{SU_m soc'_{m,t+1}} \quad \text{full}$$

The derivative soc' is always positive since we cannot increase/decrease the charge by discharging/charging. Thus the sign of C' values must be the same. Furthermore, $b_{m,t} = 0$ since the battery is full at interval t and $soc'_{m,t} = 0$ as its result. This means that the signs of C'_{t-1} and C'_{t+1} are opposite, contradicting with the first equation, proving that they must be either full or transient at the same time. Extension of the proof for empty state and power limit cases follow similarly. Note that this is not a requirement for the system to operate, but rather the condition of optimal operation. Even though our solution considers heterogeneous battery chemistries and sizes, under real operating conditions, this requirement might not be satisfied due to hidden constraints or model irregularities, resulting in suboptimal operation. However, under our stated assumptions, the provided solutions are guaranteed to converge while satisfying this requirement. This concept has a similar precedent applied at a smaller scale in every cell of the battery [40] commonly used in battery management systems. Furthermore, even though this solution appears to neglect degradation at first, degradation is in fact inherently present within the SU_n capacity. As a battery degrades, SU_n decreases, resulting in the most degraded battery to be used less and the least degraded one to be used more. To show this, we created a scenario with two identical batteries, except the

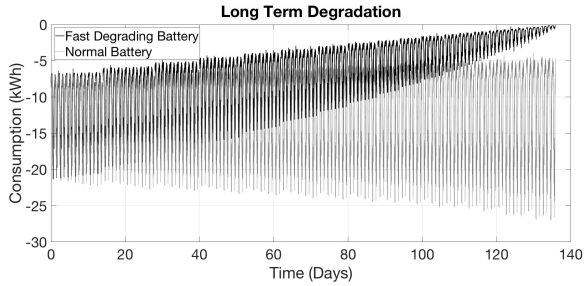

Figure 2. Long term degradation inherently present within the solution.

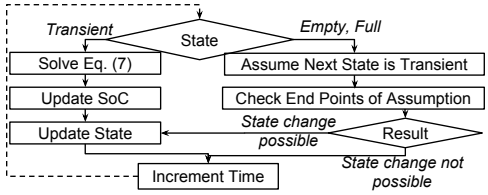

Figure 3. Algorithm flowchart for the centralized solution.

degradation coefficient of one of them has been increased by 25x. The long term solution is shown in Figure 2. It can be seen that the solution relies less on the fast degrading battery and more on the normal battery as the capacity fades in time.

Since each battery enters the full/empty state at the same time, the transient region ($\lambda = 0$) must ensure that the accumulation of charge reaches full/empty state at the same time as all batteries. The centralized solution directly follows this concept. If a battery is empty/full, the next step can either be charging/discharging or staying idle at the same state. Once the battery controller leaves a full/empty state, the optimal solution is obtained by $\lambda = 0$ until it reaches another full/empty state. Since each full/empty state is dictated by the KKT conditions, the solver must make sure that the end of a transient period ends up in a full/empty state that satisfies the KKT conditions. So, at the beginning of a full/empty state, the solver assumes virtually that a transient period can start. The transient period is calculated using (10) for all batteries at each time step, until an empty or full state is reached. The solver then checks whether the result satisfies the KKT conditions in (10). If it does, the initial assumption of transient region is correct and the transient region becomes the actual solution for the next time step. If not, the batteries stay idle for a single interval. This process is repeated until the horizon is reached. The resulting computational complexity is $O(N^2)$, meaning that the number of iterations required for the solution is upper-limited by the square of the time horizon. Note that this is the same complexity as a matrix multiplication. The flow chart of the centralized solution is shown in Figure 3.

Since the solution is based on a finite horizon, it has two methods of applicability in practice: 1) the algorithm is executed once for a long horizon to get the optimal solution for long term planning; 2) MPC, where the algorithm is executed at each time interval based on the predicted horizon values and dynamically updated at the next decision interval.

IV. Optimal Distributed Nonlinear Battery Control

The centralized solution is easily convertible to a coordination based distributed solution by construction. The distributed solution has multiple advantages over the centralized solution: 1) Computational complexity is reduced by an order of magnitude. All steps performed by the centralized solution are divided between all battery controllers in a fair manner; 2) No initial system charting is required. Battery related information is only used by the battery itself; 3) The cost coordinator, possibly implemented by the utility company, can close its cost model to the users. An energy sharing neighborhood or microgrid can minimize its utility bill using this solution.

To formulate the distributed solution, we leverage the requirement for the optimal solution: batteries must be in the same state at the same time due to (10). This requires that any transient region starts from an empty/full state and end at another empty/full state synchronously across all batteries. Even though this seems counter-intuitive from a heterogeneous degradation point across batteries, the degradation is inherently present within SU_n in (10), resulting in a more degraded battery to be used less. To achieve this condition, the charged or discharged energy by each battery at each interval must have the same effect on their total capacities:

$$\gamma_t \triangleq soc_n(\text{bat}_{n,t}) = soc_m(\text{bat}_{m,t}), \forall n, m \qquad (11)$$

The ratio, γ_t, is a single value to be satisfied by all batteries within an interval. We use this property to create three distributed negotiation based solutions. All solutions use steps similar to the centralized solution. At each interval, if the batteries are at an empty/full state, they assume that a transient region is possible. The battery power levels are then computed using (10) and (11), until an empty or full state is reached. The solution checks whether the sign of (10) is satisfied at the end points. If it is, the solution uses the assumed transient region, otherwise all batteries stay idle for a single interval. All steps require consensus between the batteries, where the power level of each battery must be solved satisfying (10) and (11). We present three negotiation schemes to solve (10), while automatically satisfying (11): 1) Circular negotiation ring that has a convergence rate independent of the number of batteries, 2) Mean circular negotiation ring, which converges very quickly for a small number of batteries, 3) Bisection method that has a convergence rate independent of the battery capacities, providing an upper bound to all. All solutions guarantee in a distributed way that all battery states are synchronous with each other and are determined such that (10) is solved in their respective regions of convergence.

A. Circular Negotiation Ring

Based on a circular communication pattern between the batteries, this solution requires a fully connected graph with a minimum node degree of 2. Since the batteries are connected to the grid and the grid is a fully connected structure, this requirement is satisfied under most circumstances. Each battery starts with an initial consumption guess (e.g. set to the previous consumption value). At each negotiation step, every

battery sends its consumption value and their current $\gamma_{n,t}$ ratio calculated using (11) to the next battery. The receiving battery updates its own consumption based on $\gamma_{n,t}$ such that $\text{bat}_{n,t} = soc_n^{-1}(\gamma_{n-1,t})$. The result is concatenated to the consumption values received from other batteries and sent to the next battery. When the initializing battery receives the results of the current iteration, it either calculates C'_{t+1} by itself if the cost function is known, or communicates with the pricing node (e.g. the utility) for C'_{t+1}. The cost values are used for the next guess value and the next iteration starts.

Convergence: The solution starts by using the γ ratio of the previous battery to obtain its own consumption, given by:

$$\text{bat}_{n+1,t} = soc_{n+1}^{-1}\left(soc_n(\text{bat}_{n,t})\right) \tag{12}$$

This chain equation has a closure at the initial node to calculate cost and the whole system becomes a fixed point equation, solvable by fixed point iteration:

$$\text{bat}_{1,t} = C'^{-1}\left(\text{bat}_1, soc_n^{-1}\left(soc_1(\text{bat}_{1,t})\right), \ldots\right) \tag{13}$$

We use the following theorem for region of convergence:

Theorem 4.1: Given a fixed point iteration, $x_{t+1} = \text{sys}(x_t)$, where $\text{sys}(x)$ is a continuous function, the solution converges to a unique fixed point if $\text{sys}(x)$ has bounded input $[L, U]$ and maps it to the same bounded output $[L, U]$.

Proof 4.1: If $\text{sys}(L) = L$ or $\text{sys}(U) = U$, then the fixed point is found. Otherwise, $\text{sys}(L) - L > 0$ and $\text{sys}(U) - U < 0$ state that there must be a point satisfying the equation between L and U, due to intermediate value theorem.

In our case, if C'^{-1} is continuous and stays within the bounds of the battery energy limits, the iteration converges. We continue with Banach's Fixed Point Theorem to bound the convergence rate. We first define contraction mapping:

Theorem 4.2: Let T be a mapping from $X \to X$, where X is the input set in metric space. T is called a contraction mapping if $d(T(x), T(y)) \leq kd(x, y)$ where $x, y \in X$ and $0 \leq k < 1$.

Theorem 4.3: Let $x_{n+1} = T(x_n)$ be a fixed point iteration and T a contraction mapping. Rate of convergence is bounded by $d(x^*, x_n) \leq \frac{k^n}{1-k} d(x_1, x_0)$, where x^* is the solution.

For our case the magnitude of the Jacobian is:

$$\max_i \frac{soc'_i(\text{bat}_{i,t})}{soc'_1(soc_1^{-1}\left(soc_i(\text{bat}_{i,t})\right))} \simeq \max_i \frac{SU_i}{SU_1} \tag{14}$$

This means that the convergence rate is upper limited by the maximum capacity ratio of any two batteries. The ratio of 1 is obtained when any two batteries have the same capacity values and the solution will diverge. But, as long as the batteries are not the same, the iteration converges exponentially by the ratio of their capacities independent of the number of batteries.

B. Mean Circular Negotiation Ring

Similar to the circular negotiation ring, this solution also requires that each battery sends its consumption and γ_t ratio to the next battery during every iteration cycle. The main difference is in the calculation of γ_t. Rather than using the γ ratio of the previous battery directly to calculate its consumption, an additional parameter of average γ, γ_m, from the previous iteration is sent and used to determine the consumption: $b_{n,t} = soc_n^{-1}(\gamma_m)$. The extra averaging enables an order of magnitude faster convergence for a small number of batteries.

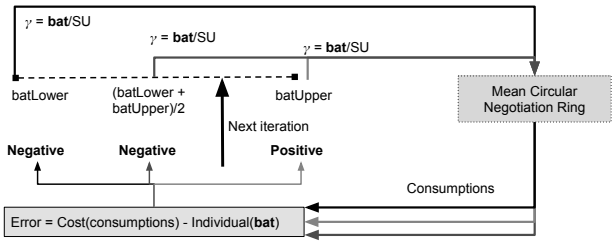

Figure 4. The bisection method workflow illustration.

Convergence: Each battery uses the average γ_m value from the previous iteration: $\text{bat}_{n,t} = soc_n^{-1}(\gamma_m)$. After each battery calculates its own consumption, the closure is achieved at the initializing node to calculate the mean ratio for the next iteration, γ'_m, where N is the number of batteries:

$$\gamma'_m = \frac{1}{N}\sum_{n=1}^{N} soc_{n,t} = \frac{soc_{1,t}}{N} + \gamma_m \frac{N-1}{N} \tag{15}$$

Combining this expression with the consumption we obtain:

$$\text{bat}_{n,t} = soc_n^{-1}\left(\frac{soc(\text{bat}_{1,t})}{N} + \frac{N-1}{N}\gamma_m\right) \tag{16}$$

The Jacobian is either dominated by $\frac{SU_n}{NSU_1}$ or $\frac{N-1}{N}$, depending on the configurations. In the event of a large number of batteries, the second term dominates and the convergence rate slows down as the number of batteries increases. This is a disadvantage compared to the previous algorithm, but for a low number of batteries and the case of identical batteries, the first term dominates and we have an order of magnitude faster convergence than the first method. A region of divergence exists for a small area, due to the discontinuous nature of: $soc''(x) = \alpha(\alpha-1)x^{\alpha-2}/SU$ for $x < 0$. This discontinuity in the calculation of R_n, causes the negotiation to oscillate around its neighborhood, defined by: $\lambda_n \alpha_n (\lambda_n - \text{load}_n)^{\alpha-1} \leq 1 \cap \lambda_n \leq \text{load}_n$. Although this region corresponds to small discharge powers of a few watts for typical configurations, the Bisection method solves these problematic regions.

C. Bisection Method

This iteration scheme is a modification of the mean circular negotiation ring method. The iteration is not determined by a reevaluation of previous values, but by partitioning using previous results, illustrated in Figure 4. The communication among batteries remains unchanged, where the consumption is calculated using γ_m. The difference is that the initial battery does not compute the next iteration consumption directly using the inverse of the cost function, but starts with the widest consumption interval possible: the upper and lower power limits. To satisfy optimal conditions, the individual constraint function must be equal to the total cost function in (8). The difference between them is considered the error in this case. Due to the mean value theorem, the solution in the viable region must have an error value of zero and its neighboring points must have opposite signs. The bisection method uses this knowledge to partition the valid consumption range into smaller regions with opposite signs. Since the range is fixed, the number of partitions and convergence rate are also fixed.

Convergence: Since the batteries are power constrained, the viable region can only be partitioned into finite subregions, upper limiting the number of iterations. For an error tolerance of δ, the number of iterations can be obtained as $\log_2(U - L)/\delta$. For example, a battery with power limits of $\mp 150W$ converges in 8 iterations for a tolerance of $1W$.

V. Results

A. Experimental Setup

We consider multiple use-case scenarios to compare our control algorithm. Our battery model is verified against NASA battery prognostics repository in [39] for Lithium-ion batteries. The repository contains various experiment scenarios and physical measurements cycling batteries until their capacity is reduced below the industry standard of 80% of their original capacity. We simulated the same scenarios using our model and compared our SoC and SoH estimates with the measurements. These scenarios contain 3 different ambient temperatures, 3 levels of output power and various levels of depth of discharge. Our model captures the nonlinear SoC behavior with less than 2% error and the nonlinear SoH degradation with 1.6% error. In contrast to our model, linear models in the literature don't consider the nonlinearity of SoC and ignore the degradation.

For comparison purposes we have selected the widely used heuristic of load following and a recent algorithm in the literature [22] that provides a linear optimal centralized and two decentralized solutions. The linear algorithm in [22] is used for both single trajectory calculation and MPC separately. Load following algorithm discharges the battery as the inverse of the load, such that their summation is constant. In all cases except the voltage deviation studies, the load profile is a residential building at the University of California, San Diego (UCSD) that houses 350 students to showcase the applicability of our solution for a single building. The profile has a typical trend, where the peak occurs in the evening after classes end and a smaller peak in the morning before classes start. All algorithms have a solution horizon of 24 hours. MPC solutions are recalculated every 15 minutes. The Bisection Method form of our algorithm with a single trajectory is used due to constant iteration performance, even though all forms would have converged to the same optimal result.

The cost function is a combination of time of use pricing and quadratic pricing. Time of use pricing is one of the most widely used electricity tariff in residential buildings. We use values from San Diego Gas and Electric (SDGE) residential rates [41]. A quadratic pricing profile is widely used for electrical stability based studies [22]. Note that our algorithm is guaranteed to provide the optimal solution for any convex cost function, including time of use and multi-tier functions. The quadratic function is selected since the quadratic nature punishes the user for high power values, incentivizes a flatter profile and allows us to do a fair comparison with [22], designed for quadratic pricing. The cost parameters were obtained by fitting a quadratic polynomial to multi-tier SDGE prices: $0.016\ \$/kWh^2 p^2 + 0.096p\ \$/kWh$, where p is the total energy consumption in a time step. Each time step is 15 minutes.

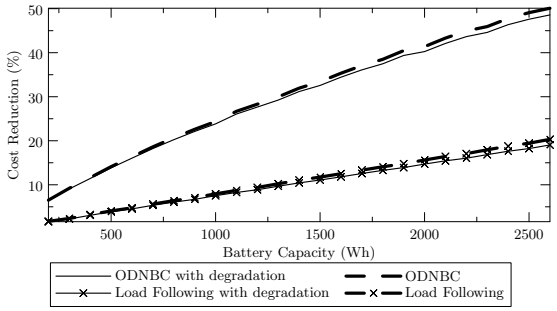

Figure 5. Cost reduction in electricity bill for ODNBC and load following.

We analyzed two scenarios in MATLAB: 1) we study how the number of batteries affect the total electricity cost, 2) how the capacity of the batteries affect the total electricity cost. In both studies, the degradation cost and electricity cost are studied separately.

B. Effect of Battery Capacity on Cost Reduction

For the first case scenario we use a single battery and change its capacity to obtain cost reduction sensitivity with respect to the battery capacity. We compare our method with the no battery case and load following heuristic. Two different cost reduction values are studied: 1) decrease in electricity cost, 2) decrease in electricity cost adjusted by the battery degradation. To obtain the second metric, we add the degradation in the battery capital as an additional cost for using the battery. We set a linear dependence between the capital cost of the battery and its capacity [42] as $\$500$ per kWh capacity. The cost reduction and the degradation effect results are given in Figure 5. The figure shows that our algorithm, denoted as ODNBC, outperforms load following by up to 30% and results in a cost reduction of up to 50%. The degradation cost results are slightly higher for ODNBC, because the optimal solution requires the battery to be discharged over a longer time.

C. Effect of Number of Batteries on Cost Reduction

Our second case study is based on the same consumption profile and cost function as in the previous study. In this case, we hold the total capacity of multiple batteries constant and change their individual capacities to understand the cost reduction dependence on the number of batteries used. To show the difference between the different solutions, a 24 hour portion of the optimal solution for a single battery and 32 batteries with equal total capacities of 2000Wh is shown in Figure 6. The results for cost reduction and degradation in Figure 7 show that as the number of batteries increases, the cost and degradation performance of the solution improves. As the batteries get smaller, their power consumption and the effect of nonlinearities also decrease, enabling a higher effective total capacity, hence a higher cost reduction and lower degradation.

D. Comparison with Linear Optimal Methods

We compare our algorithm against 3 algorithms from recent state-of-the-art work in [22]. The centralized optimal algorithm

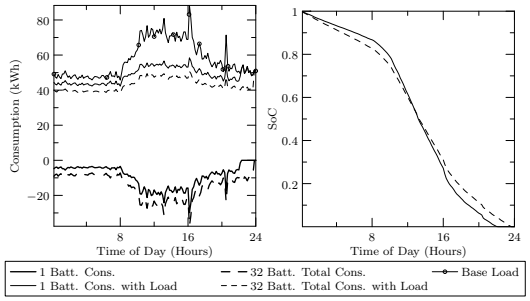

Figure 6. 24 hour solution time series for single battery and 32 batteries.

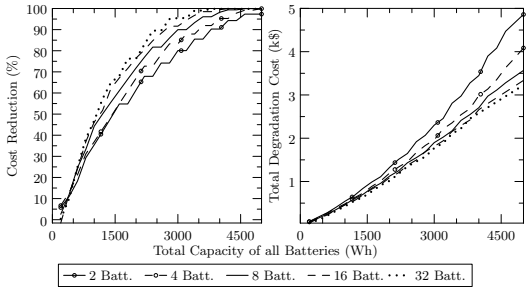

Figure 7. Effect of number of batteries on cost reduction and degradation.

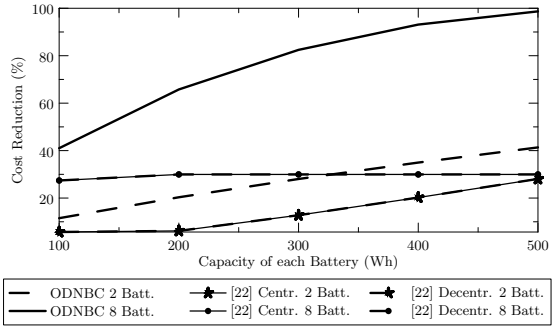

Figure 8. Percentage reduction in cost compared to the bateryless case.

uses QP to solve the system of batteries. The decentralized algorithm uses QP for each battery to get a solution for its local load separately. The optimality is not guaranteed and deviates from the global optimum for batteries with different characteristics. The third algorithm, a novel market maker MPC is a coordinated solution, where the coordination is achieved by a dynamic price. The optimality and convergence are not guaranteed. All parameters for the algorithms were obtained from [22], whereas the battery model was substituted with our nonlinear model. The reduction in cost relative to the no battery case is shown in Figure 8. The results show the significant error between the linear optimal algorithm and our nonlinear optimal solution. There are two factors: 1) negligible linearization errors at each interval due to the nonlinearity in the SoC function as given in (10); 2) accumulation of linearization errors leading into a wrong decision making. The accumulation of small errors in the memory of the battery model causes it to change states prematurely. An example is illustrated in Figure 9. During a discharge period, nonlinearity causes the battery to discharge slightly less than the linear

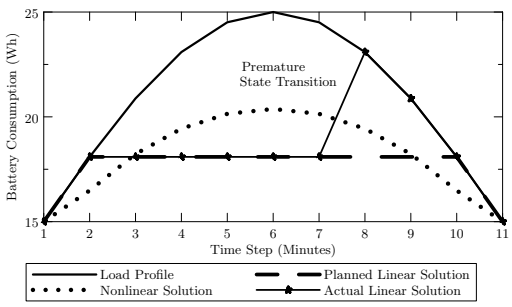

Figure 9. Example of linear model assumption leading to premature state transition.

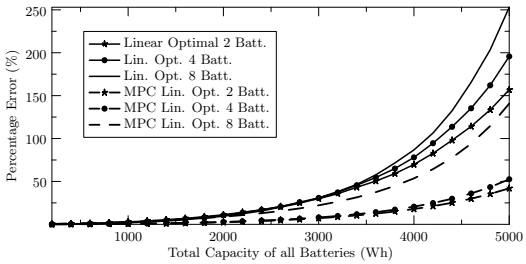

Figure 10. Error of linear model solutions, compared to our optimal solution.

solution, causing it to last longer; whereas the linear solution assumes that the battery will last longer according to its model, causing premature transition to empty state.

To further study this error caused by nonlinearity, we measure the error between the linear optimal solution and our nonlinear optimal solution for a flat load profile. In this case, we also add the MPC usage of the linear optimal solution [22]. All results with different number of batteries are shown in Figure 10. The percentage of error is calculated by: $100\% \times (\text{Cost}_{\text{linear}} - \text{Cost}_{\text{nonlinear}})/\text{Cost}_{\text{nonlinear}}$. The results show that the linear solutions, single trajectory or MPC, have significant errors. This shows that even though the linearization error at each interval is small, their accumulation in time can cause more than a 150% error for MPC and 250% for single trajectory solution compared to the nonlinear solution. These error values increase with increasing number of batteries.

E. Voltage Deviation Comparison

We compare our control algorithm to single trajectory and MPC based linear optimal algorithms from the perspective of circuit stability. We performed a voltage stability analysis on a residential neighborhood to understand how the voltage deviation is affected by the use of batteries. The electrical circuit is taken from NREL, which represents a real neighborhood in south Los Angeles, shown in Figure 11. There are 23 houses and their load profiles are created using HomeSim, a residential energy simulator [43]. All homes contain daily appliances, PV and 20% of them contain large loads such as an EV or a pool pump. PV profiles are obtained from UCSD's rooftop PV measurements. EV profile is created using the charging profile of a Nissan Leaf. All other appliance profiles are created by HomeSim that schedules start and stop events based on measured appliance statistics. Voltage stability is

Table II
VOLTAGE DEVIATION REDUCTION RELATIVE TO DEVIATION LIMIT

N	No Batt.	**ODNBC**	Lin. Opt.	MPC Opt.
2	0 (6.9%)	28% (4.1%)	8% (6.0%)	16% (5.3%)
5	0 (6.9%)	30% (3.8%)	21% (5.8%)	19% (5.0%)
10	0 (6.9%)	45% (2.4%)	21% (5.8%)	24% (4.0%)

obtained through S^{2}Sim [44], a smart grid simulator that calculates the power flow solution using OpenDSS [45]. The battery locations are marked as B on Figure 11. The error introduced due to the aggregation of loads and generation time-series is also presented. Even though residential energy sharing is not implemented currently in practice, there is an increasing amount of research for energy sharing neighborhoods [46], [47], [48]. Three cases with $2, 5$ and 10 batteries are studied,

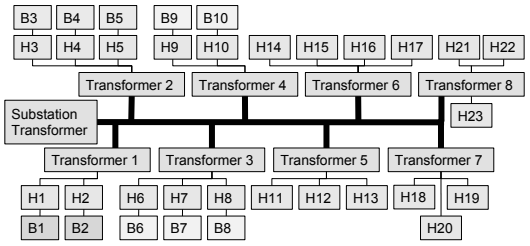

Figure 11. Neighborhood circuit with battery locations

where each battery has a capacity of $500, 200$ and 100Wh, respectively, so that the total amount of battery capacity is the same for all cases. The maximum absolute voltage deviation observed at any terminal is shown in Figure 12, where we focus on the afternoon hours as only those have significant deviation. The widely accepted maximum allowed voltage deviation is 10%. Thus we use the following metric to emphasize the voltage deviation difference *relative* to the maximum allowed value: Relative Reduction $=$ (MaxDeviation$_{\text{No Battery}}$ $-$ MaxDeviation)$/(10\%$ Limit). At peak hours, our algorithm achieves a relative voltage deviation reduction of up to 45%, helping the voltage stability significantly. Table II shows the relative voltage deviation reduction values for all cases, along with their actual deviation values in parenthesis. The results show that our algorithm has the highest reduction, lowest voltage deviation and as the number of batteries increase, the reduction improves even more, since more terminals contain batteries as stabilizing active devices. Finally, we investigate the error introduced by aggregating the loads. We look at the total line losses of the same neighborhood scenario and measure the mean absolute error compared to the actual nonlinear power flow solution. The error is normalized by the total consumption to provide a ratio of lost energy to useful energy: $\frac{1}{T}\sum_{t=1}^{T}|\frac{\text{Loss}_{\text{nonlinear}}(t)-\text{Loss}_{\text{constant}}(t)}{\text{Consumption}(t)}|$. The result is only 0.84% for our solution and 1.24% for the linear optimal solution, justifying the use of aggregation.

VI. CONCLUSION

Energy storage systems enable the on-demand dispatch of energy to compensate for generation and consumption volatility. Our optimal distributed battery control handles multiple batteries, with low computational complexity of $O(N^2)$. In contrast to previous work, we use a higher accuracy nonlinear battery model with only 2% error. We provide three iteration mechanisms to implement the distributed optimal solution with proven convergence regions and rates We show in a case study that optimal algorithms designed for a linear battery model induce an error of up to 60% in terms of cost reduction, due to the nonlinear nature of the battery. For the case of a constant load profile, we show that this error exceeds 150%.

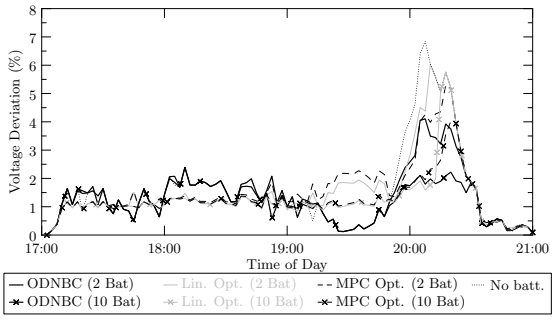

Figure 12. Absolute voltage deviation profile comparison of all solutions.

ACKNOWLEDGEMENTS

This work was supported in part by TerraSwarm, one of six centers of STARnet, a Semiconductor Research Corporation program sponsored by MARCO and DARPA and in part by ARPA-E NODES project DE-FOA-0001289.

REFERENCES

[1] J. Zhu, G. Jordan, and S. Ihara, "The market for spinning reserve and its impacts on energy prices," in *Power Engineering Society Winter Meeting, 2000. IEEE*, vol. 2, 2000, pp. 1202–1207 vol.2.

[2] Y. Agarwal, B. Balaji, S. Dutta, R. Gupta, and T. Weng, "Duty-cycling buildings aggressively: The next frontier in HVAC control," in *Information Processing in Sensor Networks (IPSN), 2011 10th International Conference on*, 2011, pp. 246–257.

[3] J. H. Yoon, R. Baldick, and A. Novoselac, "Dynamic demand response controller based on real-time retail price for residential buildings," *IEEE Transactions on Smart Grid*, vol. 5, no. 1, pp. 121–129, 2014.

[4] L. Xie, Y. Gu, X. Zhu, and M. G. Genton, "Short-term spatio-temporal wind power forecast in robust look-ahead power system dispatch," *IEEE Transactions on Smart Grid*, vol. 5, no. 1, pp. 511–520, Jan 2014.

[5] B. O. Akyurek, A. S. Akyurek, J. Kleissl, and T. S. Rosing, "Tesla: Taylor expanded solar analog forecasting," *2014 IEEE International Conference on Smart Grid Communications*, Nov 2014.

[6] D. Zhu and G. Hug-Glanzmann, "Real-time control of energy storage devices in future electric power systems," *2011 IEEE Trondheim PowerTech*, Jun 2011.

[7] A. Y. Saber and G. K. Venayagamoorthy, "Optimization of vehicle-to-grid scheduling in constrained parking lots," *2009 IEEE Power & Energy Society General Meeting*, Jul 2009.

[8] C. Lin, Y. Shiao, C.-L. Huang, and P. Sung, "A real and reactive power control approach for battery energy storage system," *IEEE Transactions on Power Systems*, vol. 7, no. 3, pp. 1132–1140, 1992.

[9] T. Ohtaka and S. Iwamoto, "Optimal allocation and pq output ratio of nas batteries for improving voltage stability in distribution systems," *2001 Power Engineering Society Summer Meeting. Conference Proceedings (Cat. No.01CH37262)*, 2001.

[10] S. Ried, P. Jochem, and W. Fichtner, "Profitability of photovoltaic battery systems considering temporal resolution," *2015 12th International Conference on the European Energy Market (EEM)*, May 2015.

[11] C. A. Hill, M. C. Such, D. Chen, J. Gonzalez, and W. M. Grady, "Battery energy storage for enabling integration of distributed solar power generation," *IEEE Transactions on Smart Grid*, vol. 3, no. 2, pp. 850–857, 2012.

[12] B. P. Roberts and C. Sandberg, "The role of energy storage in development of smart grids," *Proceedings of the IEEE*, vol. 99, no. 6, pp. 1139–1144, 2011.

[13] M. A. Elgenedy, A. M. Massoud, and S. Ahmed, "Energy in smart grid: Strategies and technologies for efficiency enhancement," in *Smart Grid and Renewable Energy (SGRE), 2015 First Workshop on*, March 2015, pp. 1–6.

[14] I. D. Serna-Suárez, G. Ordóñez-Plata, and G. Carrillo-Caicedo, "Microgrid's energy management systems: A survey," in *2015 12th International Conference on the European Energy Market (EEM)*, May 2015, pp. 1–6.

[15] S. Ci, N. Lin, and D. Wu, "Reconfigurable battery techniques and systems: A survey," *IEEE Access*, vol. 4, pp. 1175–1189, 2016.

[16] C. L. Nge, O. Midtgard, and L. Norum, "PV with battery in smart grid paradigm: Price-based energy management system," in *Proc. 38th IEEE Photovoltaic Specialists Conf. (PVSC)*, 2012, pp. 000 575–000 579.

[17] S.-J. Lee, J.-H. Kim, C.-H. Kim, S.-K. Kim, E.-S. Kim, D.-U. Kim, K. Mehmood, and S. Khan, "Coordinated control algorithm for distributed battery energy storage systems for mitigating voltage and frequency deviations," *IEEE Transactions on Smart Grid*, to be published, early Access.

[18] J. Tant, F. Geth, D. Six, P. Tant, and J. Driesen, "Multiobjective battery storage to improve PV integration in residential distribution grids," *IEEE Transactions on Sustainable Energy*, vol. 4, no. 1, pp. 182–191, 2013.

[19] K. Mets, F. De Turck, and C. Develder, "Distributed smart charging of electric vehicles for balancing wind energy," in *Smart Grid Communications, 2012 IEEE Third International Conference on*, 2012, pp. 133–138.

[20] W. Su, H. Eichi, W. Zeng, and M.-Y. Chow, "A survey on the electrification of transportation in a smart grid environment," *IEEE Trans. Ind. Inf.*, vol. 8, no. 1, pp. 1–10, Feb 2012.

[21] S. Sikkabut, P. Mungporn, N. Poonnoi, M. Phattanasak, P. Thounthong, P. Tricoli, B. Nahid-Mobarakeh, S. Pierfederici, B. Davat, and L. Piegari, "A nonlinear control algorithm of li-ion battery substation for DC distributed system," in *Power Electronics, Electrical Drives, Automation and Motion (SPEEDAM), 2014 International Symposium on*, 2014, pp. 1065–1070.

[22] K. Worthmann, C. Kellett, P. Braun, L. Grune, and S. Weller, "Distributed and decentralized control of residential energy systems incorporating battery storage," *IEEE Transactions on Smart Grid*, vol. 6, no. 4, pp. 1914–1923, 2015.

[23] B. Aksanli, T. Rosing, and E. Pettis, "Distributed battery control for peak power shaving in datacenters," in *Green Computing Conference (IGCC), 2013 International*, 2013, pp. 1–8.

[24] A. Seaman, T.-S. Dao, and J. McPhee, "A survey of mathematics-based equivalent-circuit and electrochemical battery models for hybrid and electric vehicle simulation," *Journal of Power Sources*, vol. 256, pp. 410–423, Jun 2014.

[25] Y. Zou, X. Hu, H. Ma, and S. E. Li, "Combined state of charge and state of health estimation over lithium-ion battery cell cycle lifespan for electric vehicles," *Journal of Power Sources*, vol. 273, pp. 793 – 803, 2015.

[26] J.-H. Kim, S.-J. Lee, E.-S. Kim, S.-K. Kim, C.-H. Kim, and L. Prikler, "Modeling of battery for ev using emtp/atpdraw," *Journal of Electrical Engineering and Technology*, vol. 9, no. 1, pp. 98–105, jan 2014.

[27] J. Groot, "State-of-health estimation of li-ion batteries: Cycle life test methods," Ph.D. dissertation, Chalmers University of Technology, 2012.

[28] H. Bindner, T. Cronin, P. Lundsager, J. F. Manwell, U. Abdulwahid, and I. Baring-Gould, "Lifetime modelling of lead acid batteries," Riso, Tech. Rep., 2005.

[29] B. J. S. Drouilhet, "A battery life prediction method for hybrid power applications," NREL, Tech. Rep., 1997.

[30] A. Hoke, A. Brissette, D. Maksimovi?, A. Pratt, and K. Smith, "Electric vehicle charge optimization including effects of lithium-ion battery degradation," in *2011 IEEE Vehicle Power and Propulsion Conference*, Sept 2011, pp. 1–8.

[31] A. Hoke, A. Brissette, K. Smith, A. Pratt, and D. Maksimovic, "Accounting for lithium-ion battery degradation in electric vehicle charging optimization," *IEEE Journal of Emerging and Selected Topics in Power Electronics*, vol. 2, no. 3, pp. 691–700, Sept 2014.

[32] H. Farzin, M. Fotuhi-Firuzabad, and M. Moeini-Aghtaie, "A practical scheme to involve degradation cost of lithium-ion batteries in vehicle-to-grid applications," *IEEE Transactions on Sustainable Energy*, vol. 7, no. 4, pp. 1730–1738, Oct 2016.

[33] M. Safari, M. Morcrette, A. Teyssot, and C. Delacourt, "Multimodal physics-based aging model for life prediction of li-ion batteries," *Journal of The Electrochemical Society*, vol. 156, no. 3, pp. A145–A153, 2009.

[34] R. Fu, S.-Y. Choe, V. Agubra, and J. Fergus, "Development of a physics-based degradation model for lithium ion polymer batteries considering side reactions," *Journal of Power Sources*, vol. 278, pp. 506 – 521, 2015.

[35] M. Ouyang, X. Feng, X. Han, L. Lu, Z. Li, and X. He, "A dynamic capacity degradation model and its applications considering varying load for a large format li-ion battery," *Applied Energy*, vol. 165, pp. 48 – 59, 2016.

[36] P. Ramadass, B. Haran, P. M. Gomadam, R. White, and B. N. Popov, "Development of first principles capacity fade model for li-ion cells," *Journal of The Electrochemical Society*, vol. 151, no. 2, pp. A196–A203, 2004.

[37] L. L. Lam and R. B. Darling, "Determining the optimal discharge strategy for a lithium-ion battery using a physics-based model," *Journal of Power Sources*, vol. 276, pp. 195 – 202, 2015.

[38] A. Akyurek, B. Torre, and T. Rosing, "Eco-DAC energy control over divide and control," in *Smart Grid Communications (SmartGridComm), 2013 IEEE International Conference on*, 2013, pp. 666–671.

[39] K. Goebel, B. Saha, A. Saxena, J. Celaya, and J. Christophersen, "Prognostics in battery health management," *IEEE Instrumentation & Measurement Magazine*, vol. 11, no. 4, pp. 33–40, Aug 2008.

[40] S. Chakraborty, A. Jain, and N. Mohan, "Novel converter topology and algorithm for simultaneous charging and individual cell balancing of multiple li-ion batteries," *2004 10th International Workshop on Computational Electronics (IEEE Cat. No.04EX915)*, 2004.

[41] [Online]. Available: www.sdge.com

[42] A. Sakti, J. J. Michalek, E. R. Fuchs, and J. F. Whitacre, "A techno-economic analysis and optimization of li-ion batteries for light-duty passenger vehicle electrification," *Journal of Power Sources*, vol. 273, pp. 966–980, Jan 2015.

[43] J. Venkatesh, B. Aksanli, J.-C. Junqua, P. Morin, and T. Rosing, "Homesim: Comprehensive, smart, residential electrical energy simulation and scheduling," in *Green Computing Conference (IGCC), 2013 International*, 2013, pp. 1–8.

[44] A. S. Akyurek, B. Aksanli, and T. Rosing, "S2sim: Smart grid swarm simulator," *Green and Sustainable Computing Conference (IGCC), 2015 International*, 2015.

[45] R. F. Arritt and R. C. Dugan, "Distribution system analysis and the future smart grid," in *Proc. IEEE Rural Electric Power Conf.*, 2011.

[46] W. Tushar, B. Chai, C. Yuen, S. Huang, D. B. Smith, H. V. Poor, and Z. Yang, "Energy storage sharing in smart grid: A modified auction-based approach," *IEEE Transactions on Smart Grid*, vol. 7, no. 3, pp. 1462–1475, May 2016.

[47] K. Mets, T. Verschueren, F. D. Turck, and C. Develder, "Exploiting v2g to optimize residential energy consumption with electrical vehicle (dis)charging," in *Smart Grid Modeling and Simulation (SGMS), 2011 IEEE First International Workshop on*, Oct 2011, pp. 7–12.

[48] D. T. Nguyen and L. B. Le, "Joint optimization of electric vehicle and home energy scheduling considering user comfort preference," *IEEE Transactions on Smart Grid*, vol. 5, no. 1, pp. 188–199, 2014.

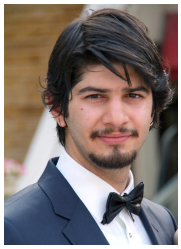

Alper Sinan Akyurek (M'13) Alper Sinan Akyurek is a PhD Candidate in Electrical and Computer Engineering at UCSD. His current work is on control and optimization of energy efficiency in the smart grid. He obtained his M.Sc. and B.Sc. degrees in Electrical and Electronics Engineering from Middle East Technical University in 2011 and 2008, respectively. Prior to PhD, he worked as a Senior Design Engineer on Wireless Networks at Aselsan, Turkey.

Tajana Simunic Rosing (SM'14) Tajana Simunic Rosing is a Professor, a holder of the Fratamico Endowed Chair, and a director of System Energy Efficiency Lab at UCSD. She is currently heading the effort in SmartCities as a part of DARPA and industry funded TerraSwarm center. During 2009-2012 she led the energy efficient datacenters theme as a part of the MuSyC center. Her research interests are energy efficient computing, embedded and distributed systems. Prior to this she was a full time researcher at HP Labs while being leading research part-time at Stanford University. She finished her PhD in 2001 at Stanford University, concurrently with finishing her Masters in Engineering Management. Her PhD topic was Dynamic Management of Power Consumption. Prior to pursuing PhD, she worked as a Senior Design Engineer at Altera Corporation.